

Propagation of a Topological Transition: the Rayleigh Instability

Thomas R. Powers¹, Dengfu Zhang^{2,*}, Raymond E. Goldstein^{1,3,†}, and Howard A. Stone²

¹*Department of Physics, University of Arizona, Tucson, AZ 85721;*

²*Division of Engineering and Applied Sciences, Harvard University, Cambridge, MA 02138;*

³*Program in Applied Mathematics, University of Arizona, Tucson, AZ 85721.*

The Rayleigh capillary instability of a cylindrical interface between two immiscible fluids is one of the most fundamental in fluid dynamics. As Plateau observed from energetic considerations and Rayleigh clarified through hydrodynamics, such an interface is linearly unstable to fission due to surface tension. In traditional descriptions of this instability it occurs everywhere along the cylinder at once, triggered by infinitesimal perturbations. Here we explore in detail a recently conjectured alternate scenario for this instability: front propagation. Using boundary integral techniques for Stokes flow, we provide numerical evidence that the *viscous* Rayleigh instability can indeed spread behind a front moving at constant velocity, in some cases leading to a periodic sequence of pinching events. These basic results are in quantitative agreement with the marginal stability criterion, yet there are important qualitative differences associated with the discontinuous nature of droplet fission. A number of experiments immediately suggest themselves in light of these results.

* Present address: Adapco, 60 Broadhollow Rd., Melville, NY 11747.

Recently, Bar-Ziv and Moses discovered the “pearling instability” of lipid bilayer membrane tubes, in which the application of laser tweezers to the membrane induces a periodic modulation in the radius [1]. Theoretical explanations [2] for this behavior invoke a tension created in the membrane by the laser tweezers. Were this an interface between two immiscible fluids, such tension would induce capillary breakup of the cylinder into droplets *via* the Rayleigh instability [3]. In the pearling phenomenon however, breakup is prevented by the membrane bending elasticity. A more striking difference is that the pearling instability propagates—the modulated state is observed to invade the uniform cylindrical region at a constant velocity. This propagation is totally unlike traditional descriptions of the Rayleigh instability [4], in which perturbations grow uniformly along the length of the tube.

In a previous publication [5], we conjectured that the viscous Rayleigh instability can propagate as well. Propagating fronts in which a new stable state invades an unstable region are a common feature of overdamped systems [6], arising in such diverse situations as reaction-diffusion systems, dendritic growth, and, more recently, type-I superconductors [7]. These previously well-studied examples all display a *continuous* evolution, in contrast to the discontinuous evolution associated with drop fission. Below we show by numerical methods that despite this fundamental difference, the Rayleigh instability of a cylindrical interface can indeed propagate. Furthermore, the coarse features of this behavior can be described by the *marginal stability criterion* (MSC), an analytical method which has found wide applicability in the simpler situations mentioned above [8].

The discontinuous evolution associated with rupture of the thread can have significant implications for the possible existence of a propagating front. As a droplet pinches off from the main body, the two tips of the broken neck recede from the pinching point; if the retracting end overtakes the front, propagation will be spoiled. Experiments on the breakup and relaxation of elongated drops suspended in an outer fluid [9] reveal that this competition depends on the relative viscosity of the two fluids. When the drop viscosity η^- is much smaller than the outer viscosity η^+ , the drop breaks before its ends have time to retract; in the other extreme, the ends retract significantly before breaking off (for long enough drops). We shall see below that when the viscosity ratio $\lambda = \eta^-/\eta^+$ is such that retraction is slow on the time scale for breakup, there is a propagating front moving with constant velocity (Fig. 1). No analytical solution is known for the complex shape evolution shown in Fig. 1. Indeed, this is the case in most examples of front propagation, where, however, the MSC nearly always provides correct predictions for front speed. In

our studies of drop breakup below we find that the front speed is rather accurately given by the linear MSC, a remarkable result in light of the strongly nonlinear, singular shape evolution behind the front. In addition to the front velocity, we compute the time between primary pinching events in the breakup of the cylinder using the MSC quantities and find good agreement with the numerical calculations.

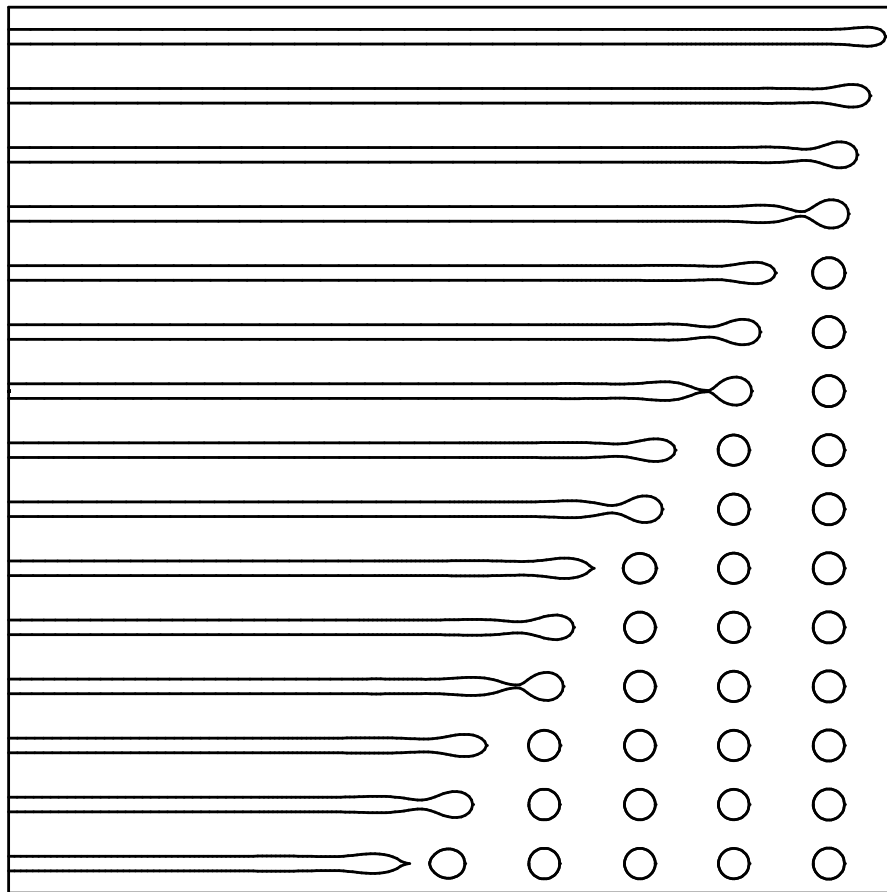


Fig. 1: Sequence of drop shapes for viscosity ratio $\lambda = 0.05$ at $t_n = 6.67n\eta^+R/\gamma$; $n = 1, 2, 3, \dots, 15$ from top to bottom. To illustrate the complete evolution, we have drawn the daughter droplets (but not the satellite droplets). However, the evolution of each connected component was computed independently of the others.

Drop evolution. We look for the propagation of the Rayleigh instability in a numerical simulation of a long, axisymmetric, approximately cylindrical drop, initially stationary and with hemispherical caps on the ends. The axis of the cylinder defines the x -direction, so that the shape is given by the surface of revolution generated by the radius $r(x)$. We work in the overdamped limit in which the inertial terms of the Navier-Stokes equations may be disregarded. Therefore, the outer and inner fluids with velocities \mathbf{u}^\pm and pressures p^\pm are described by the Stokes equations and the constraint of incompressibility

$$\eta^\pm \nabla^2 \mathbf{u}^\pm = \nabla p^\pm, \quad \nabla \cdot \mathbf{u}^\pm = 0. \quad (1)$$

Propagation in the inertial regime is complicated by the presence of dispersive capillary waves, and we leave this case and the case of net flow (like a jet) for future work. The boundary conditions at the interface S are continuity of fluid velocity $\mathbf{u}^+|_S = \mathbf{u}^-|_S$, continuity of tangential stress, and the jump in normal stress:

$$n_i(\sigma_{ij}^+ - \sigma_{ij}^-)|_S = -2\gamma H n_j, \quad (2)$$

where \mathbf{n} is the outward surface normal, H is the mean curvature, γ is the (constant) interfacial tension, and the stress tensors are $\sigma_{ij}^\pm = \eta^\pm(\nabla_i u_j^\pm + \nabla_j u_i^\pm) - p^\pm \delta_{ij}$. For an axisymmetric shape with radius $r(x)$, and with $r_x \equiv \partial r / \partial x$, the mean curvature is $H = (r_{xx}/2)(1 + r_x^2)^{-3/2} - (2r)^{-1}(1 + r_x^2)^{-1/2}$. The only important material parameters are therefore the surface tension γ and the viscosities η^+ and η^- .

Note that (2) gives rise to the *absolute* (rather than convective) instability of a stationary cylindrical interface. When the fluid velocity is zero, the pressure jump across the interface is $\Delta p = 2\gamma H$. Consider an axisymmetric perturbation in which the radius is slightly pinched to form a neck. If the disturbance is of sufficiently long wavelength, the magnitude of the curvature is increased, thus raising the pressure in the neck. Fluid is therefore forced out of the pinched region, leading to growth of the perturbation.

The challenging numerical task of solving the three-dimensional Stokes equations is greatly simplified by the boundary integral technique, in which (1) and (2) are recast as an integral equation for quantities on the interface [10]. This approach removes one spatial dimension from the problem, leading to

$$\begin{aligned} \frac{(1 + \lambda)}{2} u_j(\mathbf{y}) &= \frac{\gamma}{4\pi\eta^+} \int_S H(\mathbf{x}) n_i(\mathbf{x}) J_{ij}(\mathbf{x}, \mathbf{y}) dS(\mathbf{x}) \\ &+ \frac{(1 - \lambda)}{4\pi} \mathcal{P}.\mathcal{V}. \int_S u_i(\mathbf{x}) n_k(\mathbf{x}) K_{ijk}(\mathbf{x}, \mathbf{y}) dS(\mathbf{x}), \end{aligned} \quad (3)$$

where \mathbf{y} is a point on the interface S , $\mathbf{u}(\mathbf{y})$ is the velocity of the interface at \mathbf{y} , $\mathcal{P.V.}$ denotes the principal value, and the kernels J_{ij} and K_{ijk} are Green's functions [11].

Axisymmetry reduces our problem to an integral equation with one space and one time dimension. This equation is solved numerically by standard adaptive-grid techniques [12] to yield the interfacial velocities, and so the drop shape, as a function of time. This procedure can describe the continuous motion of the interface only; to describe the breakup of the interface we simply demand that pinching occurs whenever the radius $r(x) \leq 0.005R$, where R is the initial cylinder radius. Although somewhat arbitrary, we expect this choice for the cutoff leads to little error in the gross evolution since further decreases in the neck radius occur rapidly owing to the large velocity and curvature gradients near the pinch point. Furthermore, the size of the region in which these quantities grow large is small [13]. In any case, these same factors make it difficult to do numerical calculations when the neck approaches rupture. Once a droplet has pinched off, we neglect it in further calculations, since experience has shown the the evolution of the droplet that pinches off has little effect on the evolution of the main drop [14].

Our findings for the shape evolution are in qualitative accord with previous investigations [9]. At higher values of λ , *i.e.* around $\lambda = 10$, the evolution is dominated by retraction. As an example, Fig. 2 shows that the $\lambda = 10$ drop simply retracts and shows no sign of developing a neck in the time it takes the $\lambda = 0.1$ drop to break a few times. Fig. 3 shows a magnified view of the evolution of these droplets. Note that at a given time the radius $r(x)$ of the $\lambda = 10$ drop grows monotonically in x to its maximum value, but the radius for $\lambda = 0.1$ is modulated; these undulations are the seeds of the capillary instability.

When the outer viscosity is not too small, we can estimate the retraction speed by assuming the bulge on the drop end is spherical and balancing tension with drag [5]. This leads to a velocity that scales like γ/η^+ , since the drag is controlled by the outer viscosity [15]. This estimate only accounts for the dissipation due to the flows in the two fluids induced by dragging a spherical interface through the outer fluid; it disregards the contribution due to shape change, which become comparable when $\lambda \geq 1$. Indeed, when there is no outer fluid all the dissipation takes place inside the retracting end. The estimate is borne out by our simulations: if we take the retraction velocity to be the speed of the

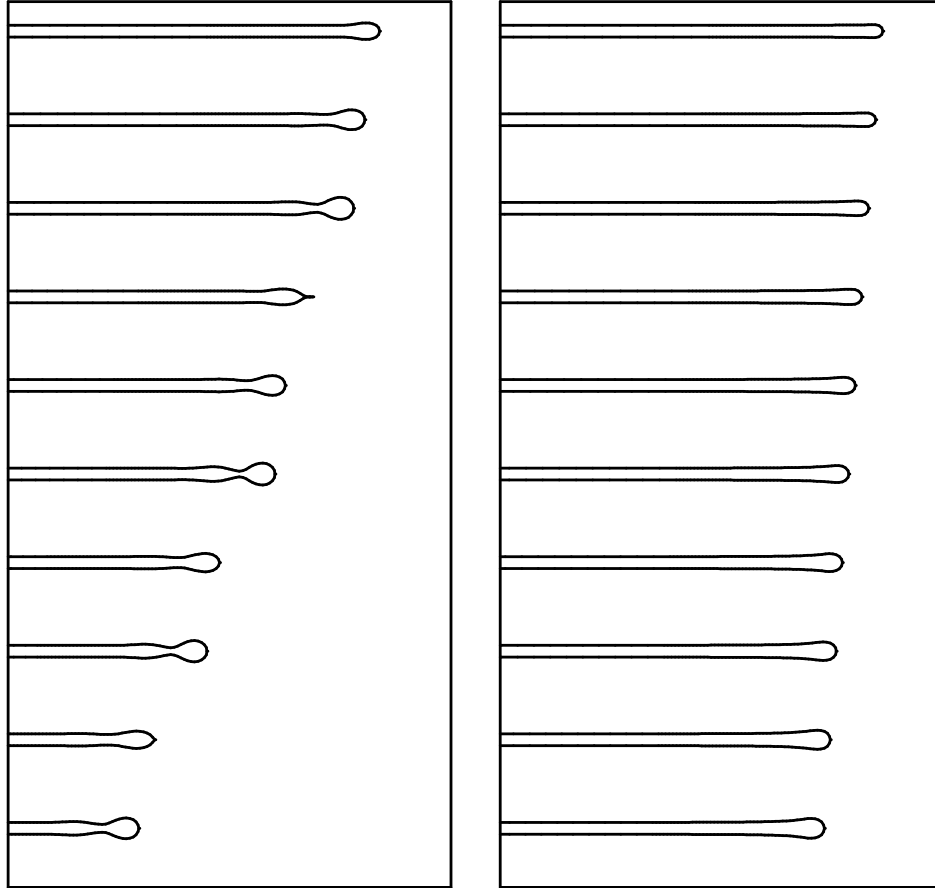


Fig. 2: Numerical results. Propagation of the Rayleigh instability for $\lambda = 0.1$ (left). Retraction-dominated dynamics for $\lambda = 10$. (right). $t_n = 6.67n\eta^+R/\gamma$, where $n = 1, 2, 3, \dots, 15$ labels the shapes from the top.

maximum of $r(x)$ nearest the end of the drop (Fig. 4), we find retraction velocities that range from $0.2\gamma/\eta^+$ at $\lambda = 0.005$ to $0.1\gamma/\eta^+$ for $\lambda = 10$.

The front region connects the uniform cylinder, which has not yet undergone the Rayleigh instability, to the growing bulge, which eventually pinches off (Fig. 4). We extract the front from the sequence of drop shapes by choosing for each shape a window with one edge such that $r(x)$ is within numerical accuracy of the unperturbed radius R , and the

other edge with $|r(x) - R|/R$ reaching a small value a^* (typically 0.1–0.15). The drop radius in this window is fit [16] with an exponential envelope times a sinusoidal function of the form $r(x) = a_1 + a_2 \exp(-q''x) \cos(q'x - a_3)$. We find that the fit parameters a_1, a_2, a_3, q', q'' do not change with small changes in the choice of fitting window or small changes in the initial shape of the ends of the drop. The front speed is the velocity of the point $x_f(t)$ for which the envelope function $a_2 \exp(-q''x_f(t)) = a^*$.

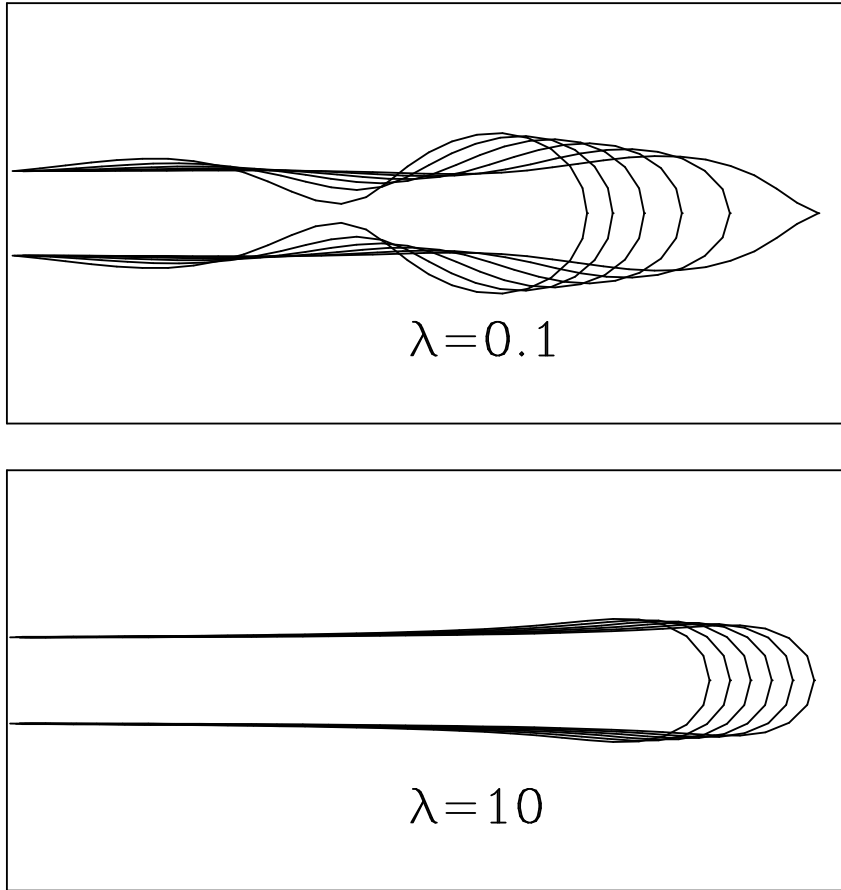


Fig. 3: Enlarged view of the droplet ends of Fig. 2 for $\lambda = 0.1$ and $\lambda = 10$. $t_n = (37.5 + 3n)\eta^+ R/\gamma$, where $n = 1, 2, \dots, 6$ labels the shapes.

Turning now to the analysis of the fronts, we find a smoothly moving front for a range of viscosity ratios, from $\lambda = 0.005$ to $\lambda = 1.0$. For example, the top graph in Fig. 5

shows the front position as a function of time for $\lambda = 0.05$. At low values of λ , around $\lambda = 0.005$ [17], the ends do not retract much before the drop pinches (Fig. 2). This is the “end-pinching” behavior described in [9]: the daughter droplets pinch off one at a time in a periodic fashion at the ends of the main drop [18]. Despite the discrete nature of these events, there is a front moving smoothly at constant velocity. We therefore interpret this end-pinching at low viscosity ratio as a front of the Rayleigh instability.

As λ increases, retraction becomes more apparent in the time it takes the droplets to break off. When λ reaches a value at which the retraction speed becomes comparable to the speed at which the pinches are spreading (around $\lambda = 1$), we find that the drop evolution can not be described as a smoothly moving front. The details of this process are complicated. For $\lambda \simeq 0.2$, the periodic behavior of the breakup ceases. The droplets that pinch off are not of uniform size and do not pinch off at a constant rate. Nevertheless, we are still able to fit the advancing profile to a front moving smoothly with constant velocity. When $\lambda > 1.0$, this smoothly propagating front behavior is lost. Around this value of λ we also observe necks that start to form at one point but then heal, leading to breakup at a different point along the drop. This behavior is reminiscent of that seen in the experiments of Tjahjadi *et al.*, who observed that a drop stretched to a cylindrical shape just beyond the critical aspect ratio for breakup does *not* break [19]. Instead, two necks form and then disappear, and the elongated drop retracts to a sphere without breaking. We can offer no explanation of this behavior, and merely note that when retraction is faster than the pinching process, there is no reason to expect the simple picture of the Rayleigh instability outlined in the last section to apply.

Front velocity and the MSC. For completeness, we review first the basic facts of the marginal stability criterion. In the leading edge of the front, the amplitude $u(x, t) \equiv r(x, t) - R$ is small and can be represented as a linear combination of Fourier modes each having the form $u(x, t) \sim \exp(\omega(q^*)t + iq^*x)$, in which $\omega(q)$, possibly complex, is the linear growth rate, and the real and imaginary parts of the wavevector $q = q' + iq''$ describe the periodicity and sharpness of the mode. The velocity of the exponential envelope of any mode is $v_q = \text{Re}\omega/\text{Im}q$. The MSC selects a unique mode q^* (and hence velocity v^*) by the condition that the envelopes of modes nearby in q neither outrun nor fall behind that of q^* . This provides two additional relationships between v and q , leading to the conditions

$$v^* = \frac{\text{Re}\omega^*}{\text{Im}q^*}, \quad \text{Im}\frac{\partial\omega^*}{\partial q} = 0, \quad v^* = \text{Re}\frac{\partial\omega^*}{\partial q}, \quad (4)$$

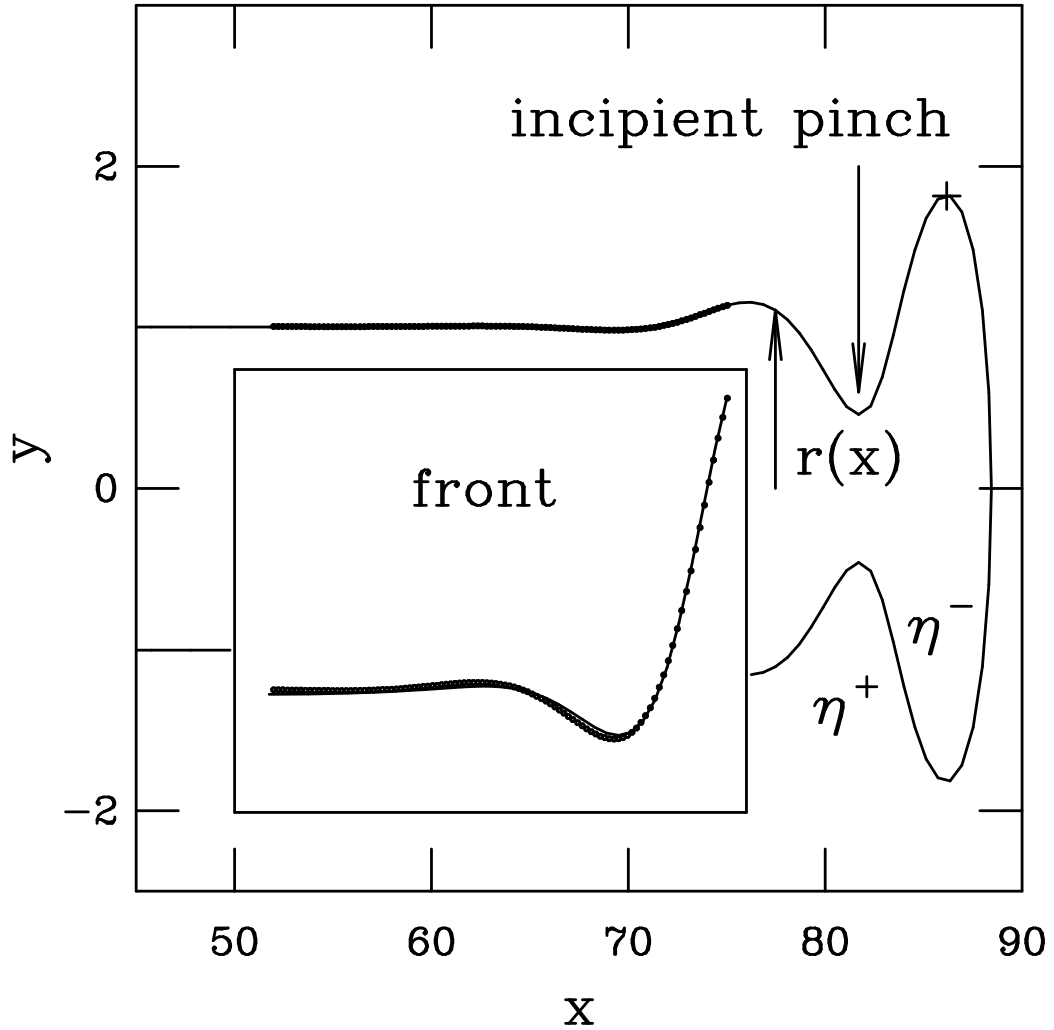


Fig. 4: A snapshot of the end of the main drop for $\lambda = 0.05$, in which the aspect ratio has been distorted to show the front more clearly. The center of the drop is at $x = 0$. The darkened line is the front region; the inset is a magnified view of this region (solid line) and a fit to the front (dotted line). The retraction speed is taken to be the velocity of the maximum marked with a plus sign.

where $\omega^* = \omega(q^*)$ [8][20]. A rigorous proof of the validity of this approach is known only for the Fisher-Kolmogorov equation [21], $u_t = u_{xx} + u - u^3$, for which it can be shown that sufficiently localized initial conditions will evolve into a front moving at a unique speed $v = v^*$ [22]. A very large number of partial differential equations have been

shown to be correctly described by this principle or its nonlinear variants [8], even when no analytic front solution is known. There is, however, no general criterion to determine when the MSC is applicable, and thus the question of its validity in this new setting of discontinuous evolution is of great interest.

The MSC quantities depend only on the growth rate ω , which is known from Tomotika's generalization [23] of Rayleigh's result to the two-fluid problem. For a cylinder of radius R , ω is a function of wavevector q and viscosity ratio λ in the form $\omega(q, \lambda) = (\gamma/R\eta^+) \Lambda(q, \lambda)(1 - q^2)$. The dynamical factor $\Lambda(q, \lambda)$, too lengthy to quote here, accounts for viscous dissipation, and the factor $\gamma(1 - q^2)$ is associated with the Young-Laplace force due to a constant-volume distortion of wave number q . Inserting this growth rate into the MSC equations (4) yields the front velocity previously derived in [5] as a function of viscosity ratio. Fig. 6 compares this prediction with our present numerical calculations.

Note that since the growth rate for the Rayleigh instability does not contain the physical process of retraction, we expect the MSC velocity to depart from the true front speed when the front and retraction speed are comparable. This may be the source of disagreement between the MSC and the numerical simulations for $\lambda \geq 0.5$. As λ is increased beyond this value, retraction becomes more important until finally the simple picture of a propagating Rayleigh instability becomes invalid. At the lower end of the viscosity contrasts we studied, the boundary integral method starts to lose accuracy; since it is difficult to quantify these errors we cannot say if this is the source of disagreement between the MSC and the numerical calculations [24].

While the front position advances smoothly in accord with the MSC picture, the behavior of the front shape encoded in the wavenumber q' and the inverse front width q'' is more complicated. We find that these quantities are not constant but rather oscillate with approximately the period of pinching; however, they are always near the MSC values. We show one example in the bottom graph of Fig. 5. We conclude that the MSC captures the gross features of the front shape but not the fine structure.

Given that we find the breakup process to be periodic in the viscosity range $\lambda = 0.005$ – 0.1 , it is natural to ask if the MSC can predict the time t_{pinch} between primary pinching events, once the transients due to the initial shape settle down. A plausible but naive starting point is to use the shortest characteristic growth time, $t_{\text{pinch}} = \omega(q_{\text{max}})^{-1}$, where q_{max} is the wavenumber of the fastest growing mode. However, it is well known that the fastest growing mode is not the mode that is selected when the MSC is applicable. In

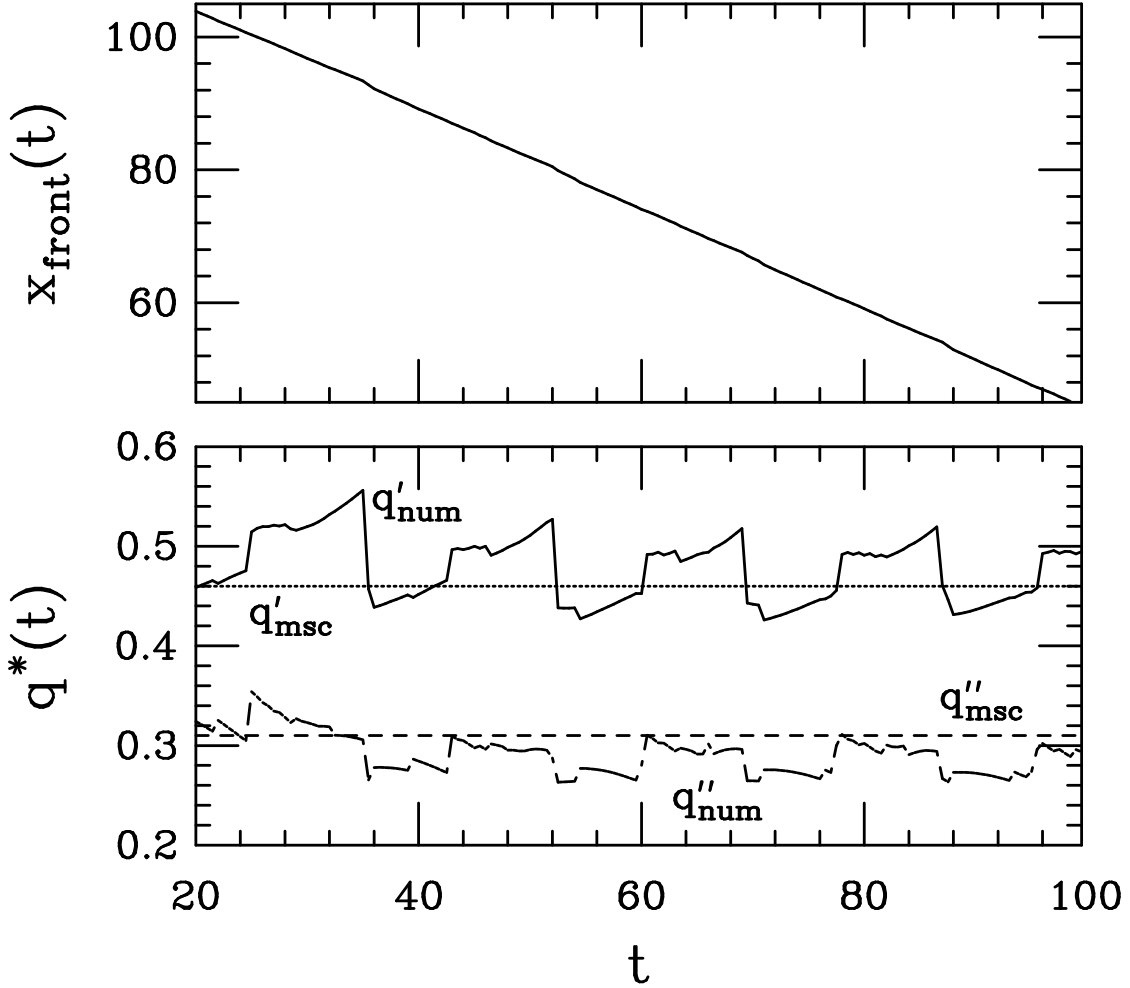


Fig. 5: Top: results of boundary integral calculations and fitting routine for front position *vs.* time. Bottom: comparison of prediction of MSC and results of boundary integral method for the initial front wavenumber q' and front width q'' . Both plots are for $\lambda = 0.05$. The simulation begins at $t = 0$; by $t\gamma/(\eta^+R) = 20$ transients from the initial shape have died out.

the standard MSC treatment, there are in fact *two* selected wavenumbers: q' , the selected wavenumber in the *leading edge* of the front, and $q_0 = \text{Im}(\omega(q^*) + iq^*v^*)/v^*$ [8], the selected wavenumber in the *saturated* pattern. Thus another candidate for the pinching time is $t_{\text{pinch}} = 2\pi/(q_0v^*)$. However, as we pointed out in [5], we do not expect q_0 to be relevant

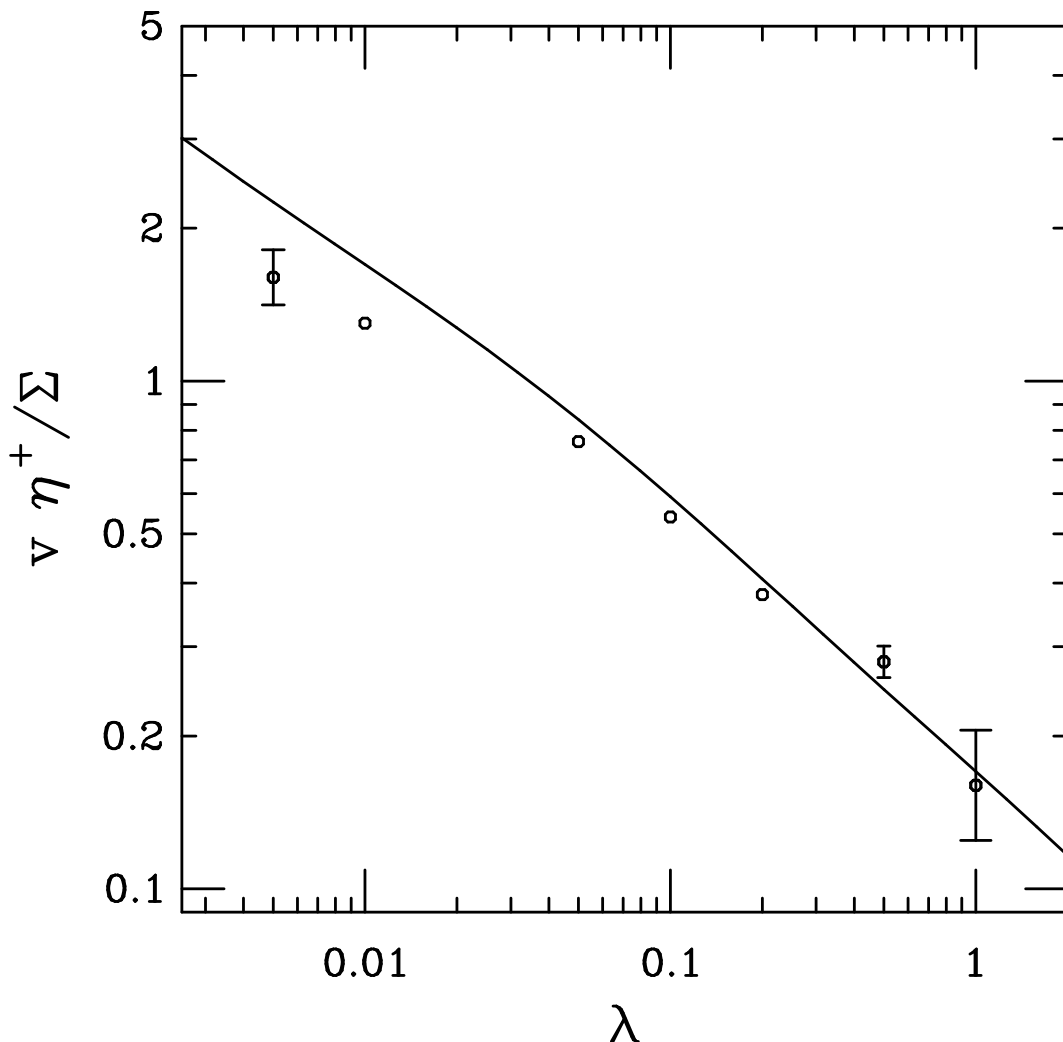


Fig. 6: Front velocity v vs. λ . The circles are the results of the numerical calculations, the line is the prediction of the MSC from [5].

to the Rayleigh problem since the saturated pattern has not continuously evolved from the leading edge of the front. Therefore we expect the appropriate wavelength to be $2\pi/q'$. In Fig. 7 we show that the numerical simulations clearly favor the relation $t_{\text{pinch}} = 2\pi/(q'v^*)$.

In conclusion, we have shown that the breakup of elongated drops can proceed *via* front propagation for the viscosity ratios in the range $\lambda = 0.005$ – 1.0 . Remarkably, despite the complex nature of the discontinuous dynamics, the marginal stability criterion gives a good description of the gross quantitative features of the shape evolution, such as the front velocity and shape, and the pinch-off time. There are many experimental systems

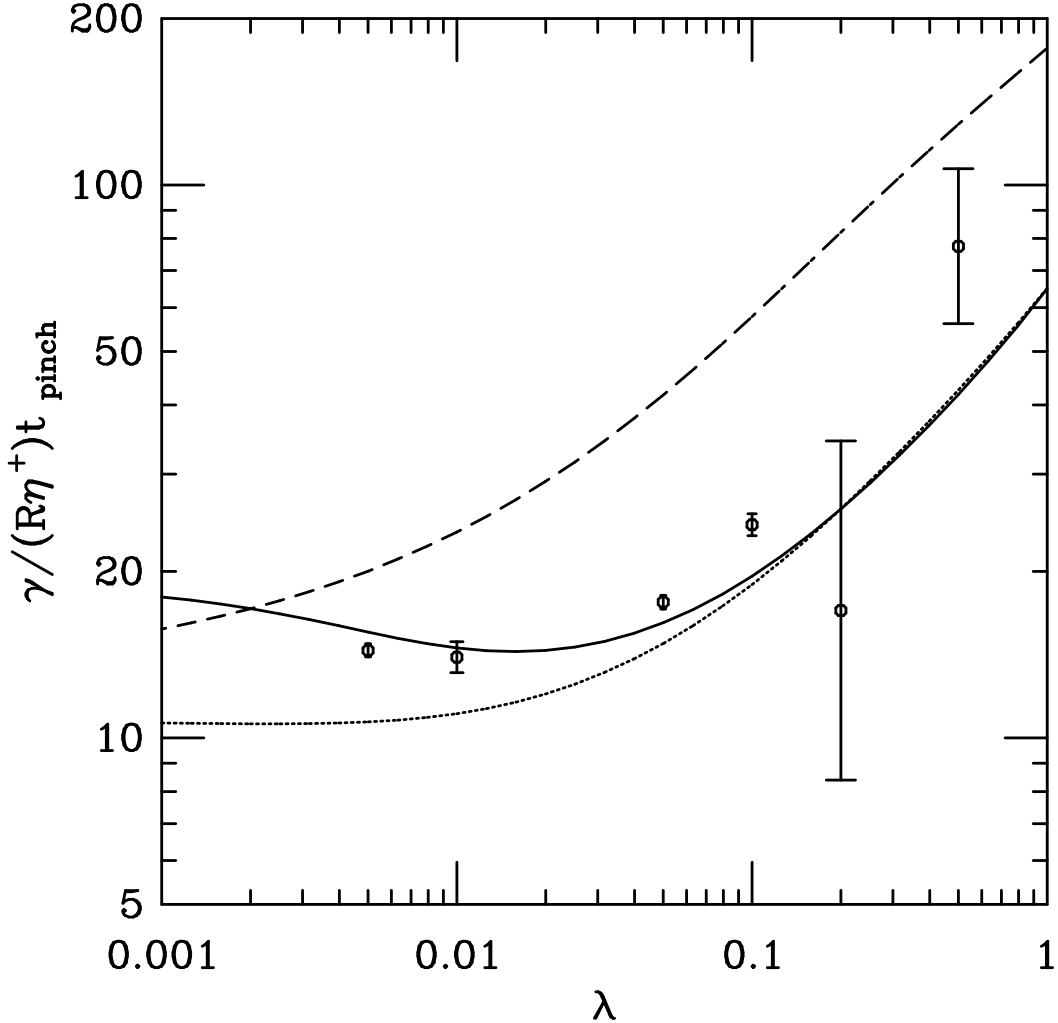


Fig. 7: Various predictions for the primary pinch time. Solid line is $2\pi/(q'v)$, dotted line is $2\pi/(q_0v)$, and the dashed line is $1/\omega(q_{\max})$. The circles are from the simulation. The breakup is aperiodic for $\lambda \geq 0.2$, leading to a distribution of droplet sizes.

which could be used to test our results. The most natural candidate is the four-roll mill, in which a planar hyperbolic flow stretches a spherical drop into a long thread [9]. When this flow ceases, the relaxation or breakup of the thread can be studied. Other possibilities are capillary bridges stabilized by electric or magnetic fields [25] or very viscous jets. Experimental confirmation of our picture of propagating topological transitions would be an important contribution to the understanding of interface motion in fluid dynamics.

Acknowledgements

TRP thanks Dartmouth College for hospitality. This work was supported by NSF Presidential Faculty Fellowship grant DMR 93-50227 (REG), and the Petroleum Research Fund (Grant No. 28690-AC9) (DFZ and HAS). E-mail: powers@physics.arizona.edu, dengfu@adapco.com, gold@physics.arizona.edu, has@stokes.harvard.edu.

References

- [1] R. Bar-Ziv and E. Moses, *Phys. Rev. Lett.* **73**, 1392 (1994); R. Bar-Ziv, T. Tlusty, and E. Moses, *Phys. Rev. Lett.* **79**, 1159 (1997).
- [2] P. Nelson, T. Powers, and U. Seifert, *Phys. Rev. Lett.* **74**, 3384 (1995), cond-mat/9410104; R. Granek and Z. Olami, *J. Phys. II France* **5**, 1348 (1995); R. E. Goldstein, P. Nelson, T. R. Powers, and U. Seifert, *J. Phys. II France* **6**, 767 (1996), cond-mat/9510093.
- [3] J. Plateau, *Statique experimentale et theorique des liquides soumis aux seules forces moleculaires* (Gautier-Villars, Paris, 1873); Lord Rayleigh, *Proc. Lond. Math. Soc.* **10**, 4 (1879); *Phil. Mag.* **34**, 145 (1892).
- [4] S. Chandrasekhar, *Hydrodynamic and Hydromagnetic Stability* (Oxford University Press, Oxford, 1961).
- [5] T. R. Powers and R. E. Goldstein, *Phys. Rev. Lett.* **78**, 2555 (1997), cond-mat/9612169.
- [6] M. C. Cross and P. C. Hohenberg, *Rev. Mod. Phys.* **65**, (1993).
- [7] S. J. Di Bartolo and A. T. Dorsey, *Phys. Rev. Lett.* **77**, 4442 (1996), cond-mat/9607023.
- [8] G. Dee and J. S. Langer, *Phys. Rev. Lett.* **50**, 383 (1983); E. Ben-Jacob, H. Brand, G. Dee, L. Kramer, and J. S. Langer, *Physica* **14D**, 348 (1985); W. van Saarloos, *Phys. Rev. A* **37**, 211 (1988); **39**, 6367 (1989).
- [9] H. A. Stone, B. J. Bentley, and L. G. Leal, *J. Fluid Mech.* **173**, 131 (1986). See also the seminal work of G. I. Taylor, *Proc. Roy. Soc. A* **146**, 501 (1934).
- [10] C. Pozrikidis, *Boundary Integral and Singularity Methods for Linearized Viscous Flow* (Cambridge University Press, Cambridge, 1992). See also A. Z. Zinchenko, M. A. Rother, and R. H. Davis, *Phys. Fluids* **9**, 1493 (1997).
- [11] The kernels in (3) are

$$J_{ij}(\mathbf{x}, \mathbf{y}) = \frac{\delta_{ij}}{|\mathbf{x} - \mathbf{y}|} + \frac{(\mathbf{x} - \mathbf{y})_i(\mathbf{x} - \mathbf{y})_j}{|\mathbf{x} - \mathbf{y}|^3},$$

$$K_{ijk}(\mathbf{x}, \mathbf{y}) = -6 \frac{(\mathbf{x} - \mathbf{y})_i(\mathbf{x} - \mathbf{y})_j(\mathbf{x} - \mathbf{y})_k}{|\mathbf{x} - \mathbf{y}|^5}.$$

- [12] J. Tanzosh, M. Manga and H.A. Stone, *Proceedings of Boundary Element Technologies VII*, C.A. Brebbia and M.S. Ingber, Eds. (Computational Mechanics Publications, Boston, 1992), p. 19.
- [13] J. Eggers and T. F. DuPont, *J. Fluid Mech.* **262**, 205 (1994); D. T. Papageorgiou, *J. Fluid Mech.* **301**, 109 (1995).
- [14] H. A. Stone and L. G. Leal, *J. Fluid Mech.* **198**, 399 (1989).

- [15] H. Lamb, *Hydrodynamics*, 6th ed., (Cambridge, Cambridge University Press, 1993).
- [16] The front parameters were determined through a nonlinear least-squares fitting algorithm [W.H. Press, B.P. Flannery, S.A. Teukolsky, and W.T. Vetterling, *Numerical Recipes in C* (Cambridge University Press, New York, 1988)].
- [17] It is well known that numerical boundary integral methods become less accurate at small λ [10]. We found that for $\lambda = 0.001$ the volume of the drop changed by about 10% during the continuous evolution.
- [18] Many of the breakup events involved smaller, satellite droplets, the analysis of which we have not pursued.
- [19] Fig. 3c of M. Tjahjadi, H. A. Stone, and J. M. Ottino, *AIChE J.* **40**, 385 (1994).
- [20] R. J. Briggs, *Electron Stream Interactions with Plasmas*, (MIT Press, Cambridge, MA 1964); E. M. Lifshitz and L. P. Pitaevskii, *Physical Kinetics* (Butterworth-Heinemann Ltd., Oxford 1981), sec. 62–63.
- [21] R. Fisher, *Ann. Eugenics* **7**, 355 (1937); A. Kolmogorov, I. Petrovsky, and N. Piskunov, *Bull. Univ. Moskou, Ser. Internat., Sec. A* **1**, 1 (1937).
- [22] D. G. Aronson and H. F. Weinberger, in *Partial Differential Equations and Related Topics*, J. A. Goldstein, Ed. (Springer-Verlag, Heidelberg) 5 (1975).
- [23] S. Tomotika, *Proc. Roy. Soc. Lond.* **A150**, 322 (1932).
- [24] There is another possible source of error. In the MSC picture, the front accelerates to the MSC velocity with a relaxation time that scales as q''^{-1} [8] [20]. Thus, when retraction is unimportant, we would expect our numerical results to lie below the MSC curve. This discrepancy should be greatest for the smallest values of λ we considered, since it is precisely those values for which q'' is getting small [5]. However, we saw no evidence of acceleration of the front in the numerical calculations.
- [25] S. Sankaran and D. A. Saville, *Phys. Fluids A* **5**, 1081 (1993).